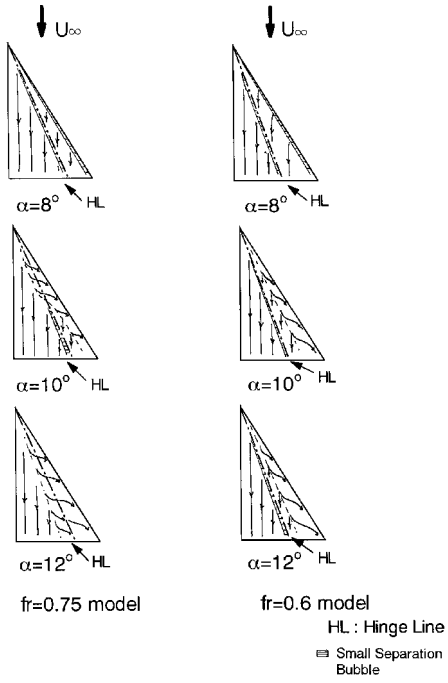

Fig. 3 Surface oil flow patterns at $fr = 0.75$ and 0.6.

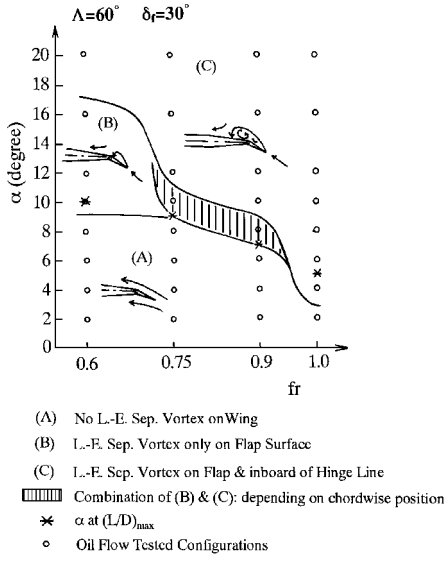

Fig. 4 Crossflow patterns for different fr.

at the flap hinge lines (at low α, all fr). Second, in regime (B) the leading-edge separation vortex is formed only over the flap surface (at $\alpha = 10$–16 deg, $fr = 0.6$ only). Third, in regime (C) the large separation vortex is formed, and its reattachment line is located inboard of the flap hinge lines (at high α, all fr). Finally, there is a fourth regime, a combination of regimes (B) and (C), in which the reattachment of the vortex occurs on the flap surface near the wing apex, but the reattachment occurs inboard the flap hinge line near the trailing edge, as was seen in Fig. 3 (at about $\alpha = 10$ deg, $fr = 0.75$ and 0.9). Figure 4 shows that the formation of a leading-edge separation vortex for the plain delta wing ($fr = 1$) is seen at $\alpha > 3$ deg for the first time when α is increased from 0 deg. However, once the flap is deflected, even though its spanwise length is only 10% ($fr = 0.9$), the angle of attack when the vortex is formed for the first time is $\alpha = 7$ deg. This indicates that a large change of flow pattern occurs even when a vortex flap that has small spanwise length is deflected ($fr = 0.9$). This may be related to the fact that the maximum L/D was attained for the $fr = 0.9$ wing when C_L was relatively small, as was shown in Fig. 2. The spanwise length of the vortex flap should be designed not only from the view point of aerodynamics but also from the results of wing structural studies.

Conclusions

In this note the effect of flap hinge-line positions over the performance of the leading-edge vortex flaps has been discussed. Differences of the vortex flap hinge-line position affect the performance of the vortex flap. The best L/D ratio is attained when the delta wing has vortex flaps with a relatively small spanwise length. The formation of leading-edge separation vortex over the wing is suppressed at relatively low angle of attack, even when the vortex flap with only a small spanwise length is deflected.

Acknowledgments

The authors express their gratitude to Y. Sunada and M. Morioka for their help in performing the wind-tunnel tests.

References

[1] Rao, D. M., "Leading Edge Vortex-Flap Experiments on a 74 deg. Delta Wing," NASA CR-159161, Nov. 1979.

[2] Rinoie, K., Fujita, T., Iwasaki, A., and Fujieda, H., "Experimental Studies of a 70-Degree Delta Wing with Vortex Flaps," *Journal of Aircraft*, Vol. 34, No. 5, 1997, pp. 600–605.

[3] Rinoie, K., "Experiments of a 60-Degree Delta Wing with Rounded Leading-Edge Vortex Flaps," *Journal of Aircraft*, Vol. 37, No. 1, 2000, pp. 37–44.

[4] Ellis, D. G., and Stollery, J. L., "The Behaviour and Performance of Leading-Edge Vortex Flaps," *Proceedings of 16th Congress of the International Council of the Aeronautical Sciences*, (ICAS Paper 88-4.5.2) 1988, pp. 758–765.

Performance Improvements of a Biplane with Endplates

N. A. Ahmed* and R. D. Archer†
University of New South Wales, Kensington, New South Wales 2052, Australia

Nomenclature

C_D = total drag coefficient of wing
C_L = lift coefficient of wing
e = span efficiency factor
Re = Reynolds number of flow based on wing chord, wind-tunnel airstream velocity, density, and dynamic viscosity
α = angle of attack or incidence

Introduction

HUMANKIND'S dream of powered flight became a reality when, in 1903, the Wright brothers demonstrated that high lift and structural rigidity of the biplane was essential to lifting man and engine into the air. However, with improvements in structural materials and technology, decreasing specific engine weights, and higher flight speeds, designers began to opt for the monoplane configuration.

In recent times, to meet the demands of an ever increasing air-cargo and transportation market, integration of any new aircraft into existing airports is becoming a significant consideration. The need for faster and more efficient aircraft with increased load carrying

Received 12 September 2000; revision received 17 November 2000; accepted for publication 26 November 2000.

*Senior Lecturer, Aerospace Engineering.
†Professor, Aerospace Engineering. Senior Member AIAA.

capacity is, therefore, growing. There is, consequently, a fresh impetus to revisit the biplane configuration concept to meet some of these new demands.

A biplane has many advantages, such as good field performance, good load carrying capability, good lift to drag ratio combined with a low wing loading, while retaining high structural strength, resulting in high lift at low speeds. A biplane also offers potential for excellent low-speed maneuverability, due to smaller span and lower inertia about the longitudinal axis, requiring less aileron which makes available more room for high lift devices.

A biplane, in general, produces higher drag than a monoplane of the same span and wing area. In this study, the possibility of incorporating endplates to a biplane is explored. The concept of adding endplates to a monoplane to reduce induced drag is not new.[1–3] The addition of endplates, however, may pose structural and vibration problems for a monoplane, but less to a biplane. The addition of endplates to an already optimized biplane may further increase the efficiency of the configuration. To date, however, this area has attracted very little attention.[4] Investigation into the improvement of the aerodynamic efficiency of a biplane with endplates, therefore, forms the basis of this study.

Experiment

Wind Tunnel and Balance

A 76-mm-diam open-return, 0.2% turbulence intensity open test section low-speed wind tunnel of the Aerodynamics Laboratory of the University of New South Wales was used in the experiments. The wind tunnel was powered by a 11-kW compound wound dc variable speed electric motor driving a fan that had eight blades. The motor was trunion mounted external to and upstream of the tunnel intake mouth. The motor speed could be varied from 200 to 1700 rpm to give a freestream velocity range of 0–30 m/s. A Betz manometer connected to a pitot static tube was used to record the wind speed.

The balance used was a simple two-axis force balance equipped with two load cells of 250-N force transducers, one measuring the side force or lift and the other the force in the direction of the flow or drag. The outputs from the load cells were amplified and fed into a TDS 360 two-channel digital oscilloscope to facilitate graphical representation of load cell output and averaging of the data. The errors calculated for the lift and drag coefficients using the balance were $\pm 1\%$, and the repeatability of each test run was approximately $\pm 0.25\%$.

Test Models and General Procedures

The design of the test model was influenced by Munk's statement[5] that if two wings of a biplane are identical, parallel, and unstaggered, the downwash produced by each wing is the same. Thus the biplane wing model consisted of two wings of constant NACA0012 cross sections. The endplate was created using a flat plate. The endplate extended upward from the lower wing to join to the upper wing. The endplate did not extend above the upper wing or below the lower wing. The two wings were produced by cutting a single wing milled from medium-density fiberboard. The resulting half span of each wing was 308 mm chord length of 154 mm, giving an aspect ratio of 2 for each half-span wing. After milling, the wings were evenly sanded before application of spray putty and enamel. Each endplate was produced from 3-mm flat steel sheet. All endplates connected the tips of the two airfoils, resulting in a cant angle of 90 deg. The endplates were cut and ground to fit the outside contour of the airfoils.

Four configurations, one without an endplate and the other three with endplates (Fig. 1) covering 100, 50, and 30% of chord lengths from the trailing edge at the tip were tested with zero decalage and zero stagger with a wing gap of one chord length. The wings were mounted to a 40-mm-diam disk plate, which in turn was connected to the two-component balance via a 2-mm-diam steel rod. The disk was rotated about its perpendicular axis to vary the angle of attack between 0 and +18 deg, and tests were conducted at a constant Reynolds number of 2.5×10^4.

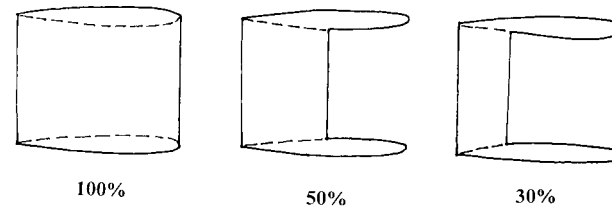

Fig. 1 Endplate configurations.

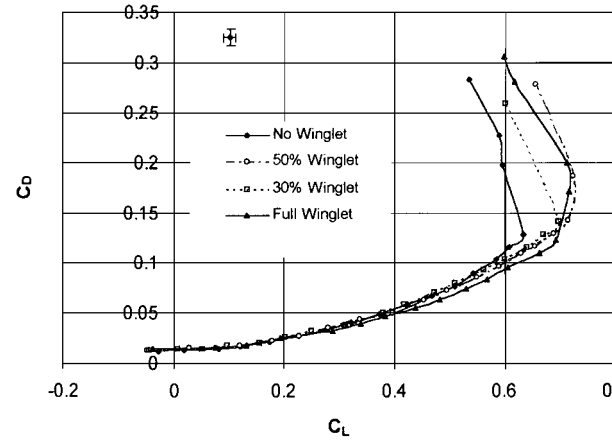

Fig. 2 Drag polar diagram, $Re = 2.5 \times 10^4$.

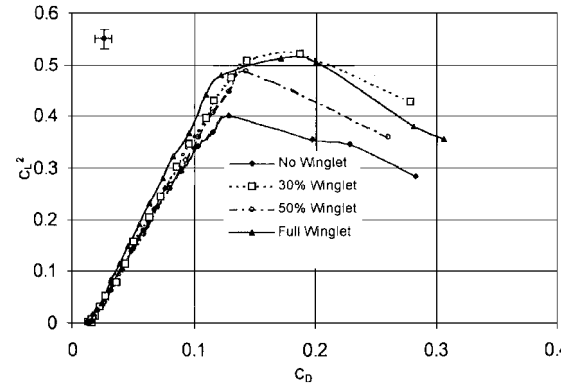

Fig. 3 Determination of span efficiency, $Re = 2.5 \times 10^4$.

Results and Discussion

Lift and drag force measurements were obtained for the four configurations, namely, the nonendplate, 100% endplate, 50% endplate, and 30% endplate configurations. To realize the comparative advantages of the endplates, results are presented in terms of drag polar and the rate of change of induced drag with lift in Figs. 2 and 3, respectively.

Drag Polar

In Fig. 2, the drag polar diagram shows that, at low-lift-coefficients, the total drag of the biplane configuration with endplates is higher than that with no endplates due to the additional profile drag; however, at $C_L > 0.3$, the reduction in the induced drag caused by the endplates begins to take effect and reduces the total C_D. For example, at $C_L = 0.6$, the full endplate configuration also shows a reduction in total drag of 16% over the nonendplate model. The maximum advantage, however, in this respect with full endplate over the nonendplate condition can be achieved when the maximum lift coefficients $C_L = 0.716$ and 0.633 are obtained for the two configurations, respectively.

However, note that the present investigation was conducted at a low Reynolds number, $Re = 2.5 \times 10^4$. Earlier work[6] suggests that although the lift curve below the stall and, therefore, the lift curve

slope and induced drag are essentially independent of Reynolds number, the maximum C_L is dependent on Reynolds number, with higher values of maximum C_L at higher Reynolds number. The minimum C_D is also found to be a function of the Reynolds number, decreasing as the Reynolds number increases. This would mean that the maximum aerodynamic efficiency, that is, C_L/C_D increases as the Reynolds number increases. These results, which are regarded as classic,[7] were conducted within $1.52 \times 10^5 < Re < 3.05 \times 10^6$. Similar trends have also been observed[8] for $3.2 \times 10^4 < Re < 9.28 \times 10^4$.

Span Efficiency

Figure 3 shows C_L^2 vs C_D. The span efficiency factor[9] e was found from the slope, $\mathrm{d}C_D/\mathrm{d}C_L^2$. The span efficiency factor for the full endplate configuration was found to be 0.74, a 22% improvement over the nonendplate configuration of 0.61. In this regard, because the slope, $\mathrm{d}C_D/\mathrm{d}C_L^2$, below the stall can be considered to be independent of Reynolds number, the benefit of endplate may be expected to be realized at full scale.

Conclusions

The results of this study demonstrate that the addition of endplates can be beneficial in decreasing induced drag and increasing span efficiency, which in turn can help increase the lift to drag ratio of a biplane configuration lifting system.

References

[1] Hoerner, S., *Fluid Dynamic Drag*, published by the author, 1965, pp. 7–7.

[2] Whitcomb, R. T., "A Design Approach and Selected Wind Tunnel Results at High Subsonic Speeds for Wing-Tip Mounted Endplates," NACA TN D-8260, 1976.

[3] Heyson, H. H., Riebe, G. D., and Fulton, C. L., "Theoretical Parametric Study of the Relative Advantages of Endplates and Tip Extensions," NACA TP 1020, 1977.

[4] Gall, P. D., "An Experimental and Theoretical Analysis of the Aerodynamic Characteristics of a Bi-Plane–Winglet Configuration," NASA TM-85815, June 1984.

[5] Munk, M., "General Bi-Plane Theory," NACA TR 151, 1922.

[6] Higgins, G. J., Diehl, W. S., and DeFoe, G. L., "Tests on Models of Three British Airplanes in the Variable Density Wind Tunnel," NACA Rept. 279, 1927.

[7] Anderson, J. D., Jr., *A History of Aerodynamics and Its Impact on Flying Machines*, 1st ed., Cambridge Univ. Press, Cambridge, England, U.K., 1997, p. 316.

[8] Bairstow, L., *Applied Aerodynamics*, 1st ed., Longmans, Green, and Co., London, 1919, p. 391.

[9] Dommasch, D. O., *Principles of Aerodynamics*, 1st ed., Pittman, London, 1953, p. 161.